Photonic-delay technique for phase-noise measurement of microwave oscillators

Enrico Rubiola

Université Henri Poincaré (Ecole Supérieure des Sciences et Technologies de l'Ingénieur de Nancy and Laboratoire de Physique des Milieux Ionisés et Applications), Nancy, France

Ertan Salik, Shouhua Huang, Nan Yu, and Lute Maleki

Jet Propulsion Laboratory, California Institute of Technology, Pasadena, California 91109

Received February 3, 2004; revised manuscript received October 23, 2004; accepted November 17, 2004

A photonic-delay line is used as a frequency discriminator for measurement of the phase noise—hence the short-term frequency stability—of microwave oscillators. The scheme is suitable for electronic and photonic oscillators, including the optoelectronic oscillator, mode lock lasers, and other types of rf and microwave pulsed optical sources. The approach is inherently suitable for a wide range of frequency without reconfiguration, which is important for the measurement of tunable oscillators. It is also insensitive to a moderate frequency drift without the need for phase locking. © 2005 Optical Society of America

OCIS codes: 120.3940, 120.5050, 060.2920, 040.5160.

1. INTRODUCTION

The ever-increasing demand for precision measurements in scientific and technological applications requires ultralow-noise, highly spectrally pure, and highly stable sources of reference signals. This is because phase, and equivalently frequency and time, are the most precisely measured physical quantities. Up until one decade ago, virtually all high-performance reference oscillators operated in the rf region of the spectrum, and any higher frequency required multiplication steps that were cumbersome and degraded the quality of the signal. In the past decade, optical techniques have overcome this obstacle, producing low-noise sources for the millimeter-wave and microwave-frequency regimes. Photonic oscillators[1,2] and mode-locked lasers[3,4] produce low-noise references in the frequency domain of tens of gigahertz and advance many applications, ranging from tests of fundamental physical laws to optical analog-to-digital converters and radar. The advent of the femtosecond optical comb[5] has completed the missing link by extending the ability to measure and characterize optical frequencies through a comparison with the microwave sources.

As the quality of the reference signals has improved, the need for measurement systems capable of precisely characterizing them has also grown. Ultralow-noise measurement systems are difficult to implement and use, and the task of the precise characterization of the noise of high-performance reference sources is relegated mostly to metrological laboratories. This is because at the level of performance of advanced standards, the measurement system is required to operate at or near the fundamental noise limits. Every source of technical noise must be carefully identified, characterized, eliminated, or reduced. Precise measurements also typically require access to an ultralow-noise reference source that is compared with the oscillator being characterized. In this conventional heterodyne approach the signals from the oscillator being tested is mixed with that of the reference in a mixer, and the output at dc (zero frequency) is measured with a spectrum analyzer. The scheme requires that the frequency of the oscillator being tested be at the same value as that of the high-performance reference with which it is being compared. This is an additional constraint for the development of low-noise sources that may have a natural oscillating frequency different from that of the reference.

Because of this, the homodyne technique for characterization of the noise of the oscillator is also used. In this approach, the signal from the source is split into two branches, one of which is delayed for decorrelation before being mixed with the first branch. For the required noise decorrelation over the (Fourier) frequency range of interest, the required delays are many microseconds long and difficult to achieve with conventional electronic techniques. Here again optical techniques can provide new capabilities for overcoming this particular barrier. The use of long fiber delays provides a low loss and a practical technique for use in homodyne schemes. A particularly desirable feature of this approach is its compatibility with optically generated microwave signals, which usually have an optical output and can be easily introduced into a fiber delay. Thus an effective scheme can be implemented that is accessible to most research laboratories interested in the characterization of the noise of high-performance oscillators.

Despite its great utility, the optically based noise-measurement scheme is not widely known in the optics community. In this paper we aim to describe this approach and provide a detailed analysis of its features and its limitations. We are interested in reference signal sources that have ultrahigh spectral purity and short

term stability. Our approach is not suitable for the measurement of long-term stability, as needed, for example, for atomic clocks that must be characterized in the time domain with a completely different measurement system.

Since the subject of rf and microwave phase-noise measurement is not necessarily a familiar one in the optics community, we begin our presentation with a discussion of the salient features of phase noise, which is also required for characterizing the time-domain stability of reference sources. We will also present a description of the heterodyne phase-noise measurement method to be compared with the homodyne technique. We provide a detailed analysis of the photonic-delay line and discuss the contributions of all sources of noise associated with various components in the measurement system. Finally, we apply the optical-delay line to characterize the phase noise of a photonic oscillator that has a performance higher than commercial measurement instruments, such as spectrum analyzers, and thus requires a high-performance test system.

2. OVERVIEW

Phase noise is described in terms of power spectral density $S_\phi(f)$ of random phase fluctuations $\phi(t)$, as a function of Fourier frequency f. This refers to the signal representation

$$v(t) = V_0[1 + \alpha(t)]\cos[2\pi\nu_0 t + \phi(t)]. \quad (1)$$

Industry reports and specifications often use $\mathcal{L}(f)$, which is defined as $\mathcal{L}(f) = \frac{1}{2}S_\phi(f)$. The amplitude noise $\alpha(t)$ and its spectrum are also of interest in many cases. An alternate quantity used to describe the frequency stability of oscillators, and closely related to $S_\phi(f)$, is the two-sample (Allan) variance

$$\sigma_y^2(\tau) = \frac{1}{2}\overline{(\bar{y}_{k+1} - \bar{y}_k)^2}, \quad (2)$$

where $\bar{y}_k$ and $\bar{y}_{k+1}$ are the fractional fluctuation $y(t) = 1/(2\pi\nu_0)(\mathrm{d}/\mathrm{d}t)\phi(t)$ averaged on contiguous time intervals of duration τ, which is the measurement time.

A model that is found useful in describing the observed phase noise of oscillators is the power-law dependence of phase noise on the Fourier frequency

$$S_\phi(f) = \sum_{i \le 0} b_i f^i, \quad (3)$$

which includes the negative powers of f including f^0 (white phase noise) to at least f^{-4} (random walk of frequency), depending on the oscillator and the observation time. Figure 1 shows the phase-noise spectrum of an oscillator, and the definitions of main terms of Eq. (3). Similar models also apply to the spectrum of frequency fluctuation $S_y(f)$ and to the Allan variance. Detailed discussions of phase noise and short-term stability are available in several references, among which we prefer the review paper of Rutman,[6] Comité Consultatif International des Radiocommunications report 580-3,[7] a book edited by Kroupa,[8] and Chapter 2 of Ref. 9. A standard[10] of the Institute of Electrical and Electronics Engineers is also available.

Among the processes of Fig. 1, we are interested mainly in the flicker of frequency, which has a slope of f^{-3} in the log–log plot of $S_\phi(f)$, and a constant two-sample variance, independent of τ.

For technical reasons, the direct measurement of $S_\phi(f)$ by means of a fast Fourier transform (FFT) analyzer is preferable for short-term fluctuations, whereas the time-domain techniques for the direct measurement of $\sigma_y^2(\tau)$ are more suitable for slower fluctuations. The breakpoint is about $f = 1$ Hz, with an overlapping of 1–2 decades. As we are interested in short-term stability, it is therefore natural to explore the frequency-domain methods, even if the final result may be reported as $\sigma_y(\tau)$.

The basic method for the measurement of phase noise in oscillators is shown in Fig. 2(a). The double-balanced mixer, saturated at both inputs, works as a phase-to-voltage converter. The gain is typically in the range of 100–500 mV/rad, depending on the device and on power. A power of 5–10 mW is usually needed to saturate the mixer. The reference oscillator is phase locked to the oscillator under test. When needed, a synthesizer makes the

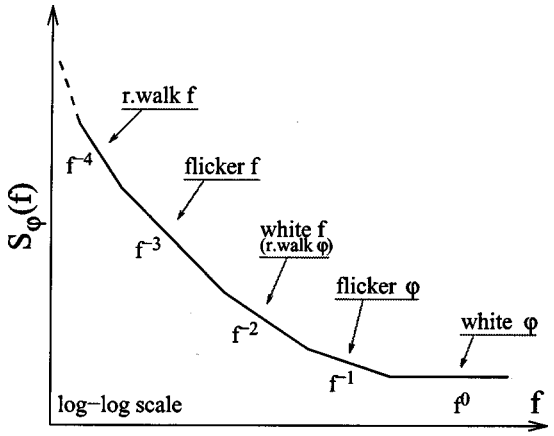

Fig. 1. Oscillator phase noise.

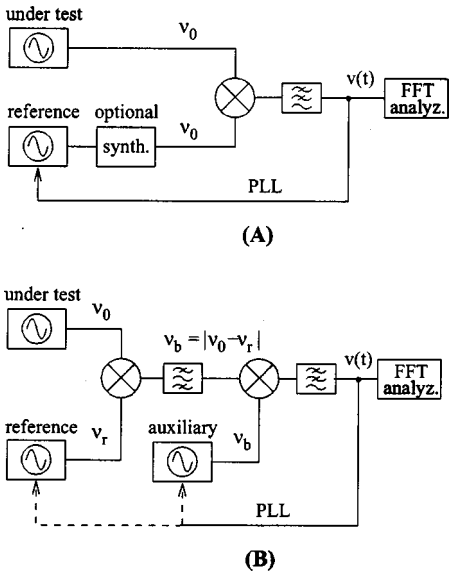

Fig. 2. Usual schemes for the measurement of $S_\phi(f)$. (A) simple phase-noise measurement, (B) beat-frequency phase-noise measurement.

nominal frequencies equal. Whereas one may be inclined to use a loose loop and to measure phase noise at frequencies higher than the cutoff, a tight loop is often preferable, because in this case the noise spectrum is multiplied by f^2. Thus, for example, the $1/f^3$ low-frequency spectrum (flicker of frequency) turns into $1/f$ (flicker of phase). As a result, the burden on the dynamic range of the FFT analyzer is strongly reduced. On the other hand, the tight loop relies upon the knowledge of the loop-transfer function, which must be measured and accounted for in order for $S_\phi(f)$ to be obtained.

Two experimental problems are inherent in the scheme of Fig. 2(a). The first is that a synthesizer is needed if the oscillator under test does not oscillate at a convenient frequency. The needed resolution is often obtained at the expense of short-term stability, which limits the measurement. The second is that microwave leakage, unavoidable in some cases, artificially reduces the phase noise and makes the measurement results incorrect. In a different context, the same mechanism is exploited to reduce the oscillator noise by injection locking.[11,12]

The beat method shown in Fig. 2(b) solves the above problems. The main point is that there is some freedom in choosing the reference, which can be an oscillator with a frequency not far from ν_0 or a lower-frequency oscillator followed by a frequency multiplier. In both cases, the short-term stability limitation of the microwave synthesizer is removed. The phase-noise measurement takes place at the beat frequency ν_b in the high frequency (HF) region, where low-noise synthesizers are available. Phase locking may be used with the reference or the auxiliary synthesizer, allowing more flexibility. In practice, ν_b is chosen to prevent any leakage from affecting the results. The scheme of Fig. 2(b) offers the highest sensitivity. Yet the problem with it is that a suitable low-noise reference must be available, at a frequency ν_r not far from ν_0, say within 50 MHz. This can be a severe constraint if one plans to measure oscillators with natural outputs in the gigahertz range. Then, in some cases, the loop gain is spread in a wide range. In short, this approach may be the only possible option for the most demanding applications, such as the case of the whispering gallery mode oscillators,[13–15] but it is difficult to design and to operate as a general-purpose instrument.

We now turn our attention to the single-oscillator (homodyne) method, in which a frequency discriminator acts as the reference with which the oscillator under test is compared. Systems based on this technique have been in use since the early use of the oscillator metrology,[16–18] yet are much older; Pound used a discriminator to stabilize an oscillator.[19] A resonator of quality factor Q is a discriminator that turns frequency fluctuations $\delta\nu$ into phase fluctuations $\phi = \delta\nu/2\nu_0 Q$. For our purpose, a resonator tunable over a wide range would be necessary. Yet the variable resonators do not have a sufficiently high stability and Q for the measurement of low-noise oscillators, and no significant progress has been made in this area since the publication of Refs. 16–18. A powerful alternative at our disposal is the photonic-delay line, which will be analyzed in Sections 3 and 4.

In this homodyne approach, the discriminator gain is proportional to the delay, but an electrical delay line is not suitable at microwave frequencies because of high attenuation. For example, a UT-141 semirigid cable (3.5 -mm diameter, polytetrafluoro-ethylene insulated) has an insertion loss of some 0.8 dB/m at 10 GHz, which limits the achievable delay to about 100 ns (25 m). Even at lower frequencies, where a longer cable has a tolerable attenuation, it was necessary to use a correlation system with two independent delay lines and phase detectors[20,21] to overcome the high background noise that results from the short delay. Needless to say, the dual-delay-line system is cumbersome, complicated, and difficult to use.

Photonic technology offers a solution, since an optical fiber typically has a refractive index $n = 1.45$ and the attenuation is as low as 0.2 dB/km at the wavelength $\lambda = 1.55$ μm. Therefore a 10-km coil exhibits a delay of 50 μs, in a reasonable size and weight (1×10^{-3} m^3 and 1 kg). Fibers show more advantages than electrical cables. First, optical power confinement is such that leakage, shielding, and grounding are no longer a problem. Then, in protected environment, there is virtually no reason for axial stress along the fiber, whereas some bending force is more likely to result from residual vibrations. The core is small (≈ 5 μm) as compared with the fiber size (125 μm) and centered along the neutral axis; thus bending the fiber has little effect on the optical path. Finally, the temperature coefficient of the refraction index n, thus of the delay, is as low as $6.85 \times 10^{-6}/\mathrm{K}^{-1}$, out of reach for cables. For reference, the room-temperature microwave oscillator that is most stable in the short term makes use of a sapphire WG (whispering gallery) resonator, which has a thermal coefficient $\mathrm{d}\nu/\nu_0 \mathrm{d}T \simeq 7 \times 10^{-5}/\mathrm{K}^{-1}$. Thus if a temperature control is needed, the control of a WG oscillator is likely to be adequate. Yet our measurements are at a much shorter time scale than the temperature-change time constant.

3. DELAY-LINE THEORY

Figure 3 shows the principle of the delay-line measure-

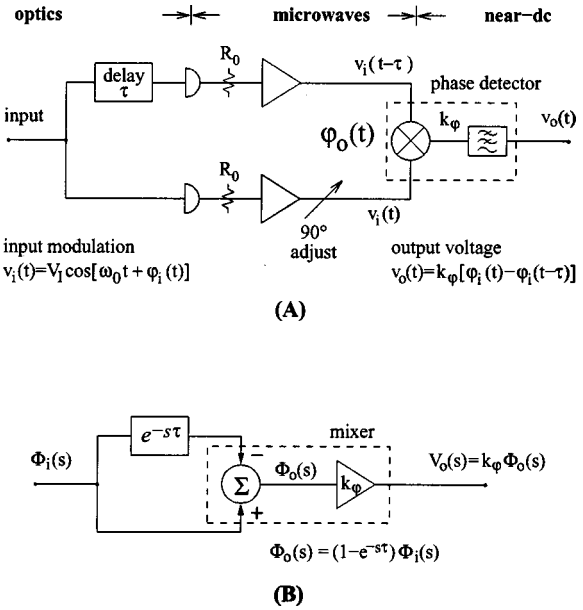

Fig. 3. Delay-line homodyne method. (A) time domain, (B) Laplace transform domain.

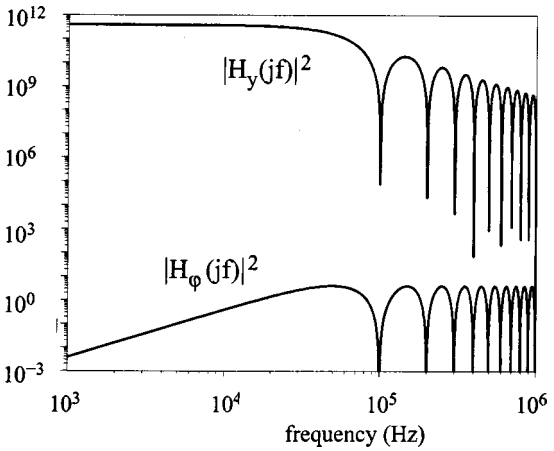

Fig. 4. Transfer functions $|H_\phi(jf)|^2$ and $|H_y(jf)|^2$ plotted for $\nu_0 = 10$ GHz and $\tau_d = 10$ μs.

ment and its equivalent in the Laplace transform domain. by inspection of Fig. 3,

$$\Phi_o(s) = H_\phi(s)\Phi_i(s), \tag{4}$$

where $H_\phi(s) = 1 - \exp(-s\tau)$. Turning the Laplace transforms into power spectra Eq. (4) becomes

$$S_{\phi o}(f) = |H_\phi(jf)|^2 S_{\phi i}(f), \tag{5}$$

where

$$|H_\phi(jf)|^2 = 4\sin^2(\pi f\tau). \tag{6}$$

The spectrum of frequency fluctuation $S_y(f)$ is related to $S_\phi(f)$ through

$$S_y(f) = \frac{f^2}{\nu_0^2} S_{\phi i}(f). \tag{7}$$

Combining Eqs. (5) and (7), we get

$$S_y(f) = |H_y(jf)|^2 S_{\phi i}(f), \tag{8}$$

where

$$|H_y(jf)|^2 = \frac{4\nu_0^2}{f^2}\sin^2(\pi f\tau). \tag{9}$$

Equation (5) is used to derive the phase noise $S_{\phi i}(f)$ of the oscillator under test. Alternatively, Eq. (7) is used to derive the frequency noise $S_y(f)$. We prefer $S_\phi(f)$, independent of how the final results will be expressed, because the background noise of the instrument appears as $S_\phi(f)$.

Figure 4 shows the transfer functions $|H_\phi(jf)|^2$ and $|H_y(jf)|^2$ for $\nu_0 = 10$ GHz and $\tau_d = 10$ μs (2-km delay line), which is typical of our experiments. For $f \to 0$, it holds $|H_\phi(jf)|^2 \sim f^2$. Fortunately, high slope processes such as flicker of frequency dominate in this region (see Fig. 1), which compensates $|H_\phi(jf)|^2$. The phase-noise measurement is therefore possible, providing that the delay τ_d can be appropriately chosen. $|H_\phi(jf)|^2$, as well as $|H_y(jf)|^2$, has a series of zeros at $f = n/\tau_d$, with integer $n \geq 1$. The experimental results are not useful in the vicinity of these zeros. At the beginning of our experiments we hoped to reconstruct the spectrum beyond the first zero at $f = 1/\tau_d$ by exploiting the maxima at $f = (2i+1)/(2\tau_d)$ (integer $i \geq 1$). This turned out to be difficult. One problem is the resolution of the FFT analyzer, as the density of zeros increases on a logarithmic scale. Another problem is the presence of stray signals in the measured spectrum, which make unreliable the few data around the maxima. The practical limit is about $f = 0.95/\tau_d$, where $|H_\phi(jf)|^2 = -16$ dB, and at most some points around $f = 3/(2\tau_d)$ between the first and second zeros.

4. SOURCES OF NOISE

The basic block for photonic phase-noise measurements is shown in Fig. 3(a). In normal operation the random phase $\phi(t)$ results from the fluctuations of the input frequency. In this section we analyze the sources of noise of the block, since $\phi_o(t)$ is acquired form the noise of electrical and optical components.

The power $P_\lambda(t)$ of the optical signal is sinusoidally modulated at the microwave angular frequency ω_μ with a modulation index m

$$P_\lambda(t) = \bar{P}_\lambda(1 + m\cos\omega_\mu t). \tag{10}$$

Here, we use the subscripts λ and μ for "light" and "microwave," and the overbar to denote the average. Equation (10) is similar to the traditional amplitude modulation of radio broadcasting, but optical power is modulated instead of rf voltage. In the presence of a distorted (nonlinear) modulation, we take the fundamental of the modulating signal, at ω_μ.

The detector photocurrent is

$$i(t) = \frac{q\eta}{h\nu_\lambda}\bar{P}_\lambda(1 + m\cos\omega_\mu t), \tag{11}$$

where $q = 1.602 \times 10^{-19}$ C is the electron charge, η is the quantum efficiency of the photodetector, and $h = 6.626 \times 10^{-34}$ J/Hz the Planck constant. Only the ac term $m\cos\omega_\mu t$ of Eq. (11) contributes to the microwave signal. The microwave power fed into the load resistance R_0 is $\bar{P}_\mu = R_0\overline{i_{\text{ac}}^2}$, hence

$$\bar{P}_\mu = \frac{1}{2}m^2 R_0\left(\frac{q\eta}{h\nu_\lambda}\right)^2\bar{P}_\lambda^2. \tag{12}$$

A. White Noise

The discrete nature of photons leads to the shot noise of power spectral density $N_s = 2qiR_0$ [W/Hz] at the detector output. By virtue of Eq. (11),

$$N_s = 2\frac{q^2\eta}{h\nu_\lambda}\bar{P}_\lambda R_0. \tag{13}$$

In addition, there is the equivalent input noise of the amplifier loaded by R_0, whose power spectrum is

$$N_t = Fk_B T_0, \tag{14}$$

where F is the noise figure of the amplifier, $k_B = 1.38 \times 10^{-23}$ J/K is the Boltzmann constant, and T_0 is the temperature. The white noise $N_s + N_t$ turns into a noise floor $S_{\phi 0} = (N_s + N_t)/P_\mu$ of $S_\phi(f)$. By use of Eqs. (12)–(14), the floor is

$$S_{\phi 0} = \frac{2}{m^2}\left[2\frac{h\nu_\lambda}{\eta}\frac{1}{\bar{P}_\lambda} + \frac{Fk_BT_0}{R_0}\left(\frac{h\nu_\lambda}{q\eta}\right)^2\left(\frac{1}{\bar{P}_\lambda}\right)^2\right]. \quad (15)$$

Equation (15) holds for one arm of Fig. 3. As there are two independent arms, noise power is multiplied by two. In addition, it is convenient to *redefine* $\bar{P}_\lambda$ as the total input power, half of which goes to the detector input. Accounting for the two arms and changing $\bar{P}_\lambda \to \bar{P}_\lambda/2$, the phase-noise floor of the entire block is

$$S_{\phi 0} = \frac{16}{m^2}\left[\frac{h\nu_\lambda}{\eta}\frac{1}{\bar{P}_\lambda} + \frac{Fk_BT_0}{R_0}\left(\frac{h\nu_\lambda}{q\eta}\right)^2\left(\frac{1}{\bar{P}_\lambda}\right)^2\right]. \quad (16)$$

Interestingly, the noise floor is proportional to $(\bar{P}_\lambda)^{-2}$ at low power and to $(\bar{P}_\lambda)^{-1}$ above the threshold power

$$P_{\lambda,t} = \frac{Fk_BT_0}{R_0}\frac{h\nu_\lambda}{q^2\eta}. \quad (17)$$

For example, taking $\nu_\lambda = 193.4$ THz (wavelength $\lambda = 1.55$ μm), $\eta = 0.6$, $F = 1$ (noise-free amplifier), and $m = 1$, we get a threshold power $P_{\lambda,t} = 689$ μW, setting the noise floor at $S_{\phi 0} = 9.9 \times 10^{-15}$ rad^2/Hz (-140 dB rad^2/Hz).

When the mixer is used as a phase-to-voltage converter, saturated at both inputs, its noise is chiefly the noise of the output amplifier divided by the conversion gain k_ϕ. Assuming that the amplifier noise is 1.6 nV/$\sqrt{\text{Hz}}$ (our low-flicker amplifiers, input terminated to 50 Ω) and that $k_\phi = 0.1$ V/rad (conservative with respect to P_μ), the mixer noise is approximately 2.5×10^{-16} rad^2/Hz (-156 dB rad^2/Hz). In practice, the mixer noise can hardly approach the noise of the microwave amplifier because of the gain of the latter. The microwave gain, hidden in Eq. (16), is not a free parameter. Its permitted range derives from the need of operating the mixer in the saturation region, below the maximum power.

Figure 5 shows the noise floor $S_{\phi 0}$ as a function of the total optical power for some reference cases.

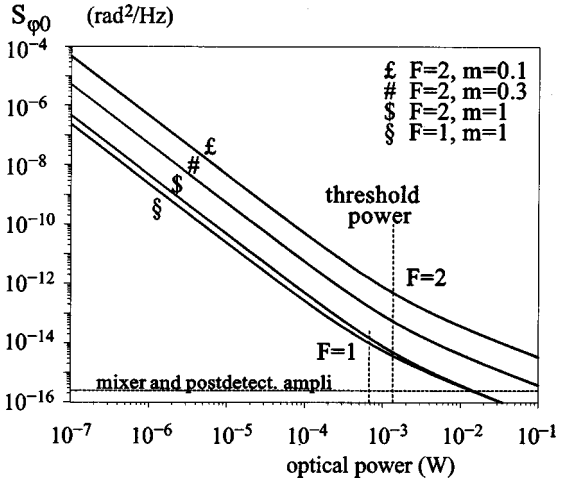

Fig. 5. Noise floor as a function of the optical power. The threshold power depends on the noise figure F.

B. Modulation Index

For a given cw laser power, the condition of maximum microwave power at the angular frequency ω_μ is that of a square wave of the same frequency that switches symmetrically between 0 and $2\bar{P}_\lambda$. This is equivalent to replacing the term $m \cos \omega_\mu t$ in Eq. (10) with a unity square wave that flips between ± 1. In our case the unity square wave can be expanded in a Fourier series truncated after the first term, because the higher harmonics ($\omega = n\omega_\mu$, with integer $n \geq 2$) are not in the passband of the microwave chain. Thus the unity square wave is replaced with sinusoid of angular frequency ω_μ and amplitude $4/\pi$. Therefore the square-wave modulation is equivalent to a sinusoidal modulation with a modulation index $m = 4/\pi \simeq 1.273$. $m > 1$ is no contradiction with the traditional modulation theory; it only means that harmonic distortion is present.

A more interesting case is that of the electro-optic modulator (EOM), which is used in virtually all photonic oscillators and as the modulator in the experiments described in Section 6. The EOM transmission, as a function of the driving voltage $v(t)$, is

$$\mathcal{T} = \frac{1}{2} + \frac{1}{2}\sin\frac{\pi v}{V_\pi}, \quad (18)$$

where V_π is the half-wave voltage of the modulator. When the driving signal is $v(t) = V_p \cos \omega_\mu t$, the transmission becomes

$$\mathcal{T}(t) = \frac{1}{2}\left[1 + 2J_1\left(\frac{\pi V_p}{V_\pi}\right)\cos \omega_\mu t + \ldots \right], \quad (19)$$

where J_1 is the first-order Bessel function of the first kind. Equation (19) derives from the zeroth term of the series expansion

$$\sin(z \cos \theta) = 2\sum_{k=0}^{\infty} (-1)^k J_{2k+1} \cos[(2k+1)\theta]. \quad (20)$$

The neglected terms "…" of Eq. (19) are higher harmonics, of angular frequency $n\omega_\mu$, integer $n \geq 2$. They also ensure $0 \leq \mathcal{T} \leq 1$. Equation (19) has the same form as Eq. (10), hence the modulation index is

$$m = 2J_1\left(\frac{\pi V_p}{V_\pi}\right). \quad (21)$$

The maximum is $m \simeq 1.164$, which occurs at $V_p = 0.586\, V_\pi$.

Harmonic distortion could be avoided if m is kept small, but there is no advantage, because harmonic distortion has no first-order effect on noise (shot and thermal). On the other hand, the optical power is limited by saturation in the photodetector. A large m is therefore the only means to increase the microwave power, thus the signal-to-shot-noise ratio. In practice, the microwave power and the dc bias of the EOM are sometimes difficult to set and maintain at the maximum modulation index. This is due to the possibility for bias drift and to the thermal sensitivity of the lithium niobate. Hence, we take $m = 1$ as the maximum, being aware that this may be somewhat optimistic.

C. Flicker Noise

The residual flicker noise derives from a number of causes for which there is no satisfactory theory. Nonetheless, based on experience and experimental facts, a model may be developed.

1. Amplifier

Phase flickering of amplifiers, as well as amplitude flickering, results from noise at near-dc frequency upconverted by the device nonlinearity. This is made evident by the simple observation that in the absence of a carrier the microwave spectrum at the amplifier output is white, i.e., constant over the entire bandwidth. Whereas a general theory does not exist, several experimental observations[22–24] suggest that different amplifiers based on a given technology tend to have about the same b_{-1} coefficient in Eq. (3), and that b_{-1} is nearly constant in a wide range of carrier frequency and power. The typical phase flickering of a "good" microwave amplifier operated well below the 1-dB compression point $P_{1\,\mathrm{dB}}$ is between $b_{-1}=1\times10^{-11}$ and $b_{-1}=2\times10^{-11}$. For example, b_{-1} of a commercial amplifier (Microwave Solutions MSH6545502) that we measured at 9.9 GHz is between 1.25×10^{-11} and 2×10^{-11} from 300 μW to 80 mW of output power. For this device, the 1-dB compression power is 160 mW.

In principle, the amplifier $1/f$ noise can be reduced with carrier suppression methods, in which only the noise sidebands are amplified. The difficulty of the absence of a clean reference with sufficient microwave power to pump the mixer has been recently solved.[25] Incorporating carrier suppression, which is well developed in the microwave domain,[26] in a photonic oscillator has been demonstrated,[27] but it is still a challenging task and we are currently studying it further.

2. Mixer Noise

There are a number of available microwave double-balanced mixers that exhibit sufficiently low residual flicker. A conservative value for the flicker coefficient is $b_{-1}<10^{-12}$. This makes the mixer noise negligible as compared with the amplifier. These low-noise mixers are available as commercial parts, without the need of individual selection. On the other hand, the double-balanced mixer must be saturated at both inputs in order for it to work properly as a phase detector. The power range is of a factor of 10 centered around (±5 dB) an optimum power of 5–10 mW. At both sides out of that range, b_{-1} increases. Furthermore, at lower power the conversion gain (0.1–0.5 V/rad) drops suddenly. This is a consequence of the exponential $i(v)$ characteristics of the internal Schottky diodes.

3. Contamination from Amplitude Noise

Mixers are sensitive to the amplitude noise of the input signal. The output voltage $v(t)$ takes the form $v=k_\phi\phi+k_\alpha\alpha$, where $\alpha(t)$ is the amplitude fluctuation defined by Eq. (1). This results from the imperfect cancellation of the voltage across the internal diodes, due to diode differences and the asymmetry of power splitting. In some cases we have measured k_ϕ/k_α as low as 5, while values of 10–20 are also common. In spite of this, amplitude noise seldom represents a problem in microwave measurements, and at most turns into a small error in the measurement of $S_\phi(f)$. Yet in photonic systems the contamination from amplitude noise can be a serious problem because of the power fluctuation of some lasers and laser amplifiers, chiefly the erbium-doped fiber amplifier (EDFA). In the radio frequency and the microwave domain, Brendel *et al.*,[28] and later Cibiel *et al.*,[29] suggests that the mixer can be operated at a point of zero sensitivity to the amplitude noise. In practice this point occurs at a few degrees off the perfect quadrature, where the residual noise and the conversion gain of the mixer are not affected. That optimal point depends on the specific mixer sample and on amplitude and frequency, for it must be determined experimentally in each case. Unfortunately, the Brendel offset method cannot be used when a discriminator is inserted in one arm. This occurs because the null of amplitude sensitivity results from the equilibrium between equal and opposite sensitivities at the two inputs. The discriminator decorrelates the signals, hence the effect of a fluctuation of the input amplitude appears at the output twice, immediately and after the discriminator delay.

4. Other Sources of Noise

The microwave photodetector contributes with its $1/f$ fluctuations, in addition to white noise. The measurement of these $1/f$ fluctuations is a challenging problem and has been reported previously only in a single instance.[30] A second source of noise is the EOM. While the physical structure makes one think that these components are less noisy than the active devices, no information has been found about their noise. A further contribution comes from the laser-amplified spontaneous emission and from the noise of the optical pump (Ref. 31, Section 10, and Appendix C). As theory does not provide clear indications about all of the above sources of noise, a pragmatic approach is necessary that consists of measuring the total noise of the microwave photonic channel.

D. Flicker Noise of the Microwave Photonic Channel

The microwave channel consists of a 1.55-μm laser diode (United Technologies Photonics UTP CW-DFB-1550) followed by an EDFA (NuPhoton NP2000GB-23B-G23-NO-58-FPIS), an EOM (Lucent X2624C) and a photodetector (Discovery Semiconductor DSC30-1K, and Lasertron QDMH-3), the same components used in the final experiments. These components are considered representative of the available ones, for similar noise is expected if similar components are chosen. The channel input is the microwave input of the EOM, and the output is the microwave output of the photodetector. The EDFA precedes the EOM instead of following it. The advantage of this uncommon configuration is that the EDFA cannot contribute to the phase noise of the microwave signal. The lower optical power, which is the main disadvantage, is not a problem in our case because the maximum power is limited by the saturation in the photodetector.

The measurement was carried out with a simplified version of the interferometric technique described in Ref. 26, at a frequency of 9.9 GHz. Basically, the system is a bridge in which the carrier is suppressed at the photode-

tector output by addition of a fraction of the signal sent to the EOM input. The noise sidebands introduced by the channel and not suppressed by the bridge are amplified and downconverted to dc by synchronous detection. This system is capable of detecting the amplitude noise and the phase noise of the channel, depending on the phase γ of the synchronous detection. With a microwave power of 0.32 W (+25 dBm) at the EOM input and an optical power of $\sim$1 mW at the detector input, the power available at the detector output was $P_\mu = 6.3\ \mu$W (−22 dBm). The maximum microwave power, obtained by an increase of the optical power, is a few decibels higher, limited limited by saturation in the photodetector. Yet in our case we had to operate the detector in the linear region; otherwise, the instability of the output power unbalances the bridge, which spoils the measurement. We simplified the measurement process by sweeping γ instead of calibrating it. The measured quantity is the noise ellipse $\phi \sin\gamma + \alpha \cos\gamma$, with arbitrary origin of γ. The semiaxes of the noise ellipse defined by the flicker measured at 1 Hz were 7.4×10^{-13} and 5.9×10^{-11}. Based on physical insight, we ascribe the maximum to amplitude noise and the minimum to phase noise, that is, 7.4×10^{-13} rad^2/Hz (−121.3 dB rad^2/Hz).

These results state that when the microwave signal of an oscillator crosses the photonic channel from the EOM input to the detector output (see Fig. 7), the phase-noise contribution of the channel is of −121.3 dB rad^2/Hz at $f=1$ Hz, of the $1/f$ type. This also includes the noise of the laser and of the EDFA. The relevant conclusion is that the flicker noise of the modulator–detector pair, including the effect of the laser noise and of the EDFA noise, is lower by a factor 30 (15 dB) than the noise of a typical microwave amplifier, thus it does not deserve more attention here.

E. Comparison of Methods

Figure 6 compares the phase-noise spectrum of some selected low-noise commercially available sources with the noise of a photonic homodyne instrument. All spectra refer to the carrier frequency of 10 GHz and to the best low-noise available option. In the case of fixed-frequency oscillators (quartz and sapphire), the spectra are converted to 10 GHz with the intrinsic property of frequency multiplication by a rational number z, that is $S_{\phi\text{out}} = z^2 S_{\phi\text{in}}$.

A synthesizer can be directly used as the reference in Fig. 2. In this case, the phase noise of the synthesizer sets the measurement limit. Phase noise can be further reduced in the lower part of the spectrum by a locking of the synthesizer to an external source. The cutoff frequency below which locking is effective depends on the synthesizer inside.

A quartz oscillator followed by a frequency multiplier can be used as the reference by use of the scheme of Fig. 2(b). Experience suggests a choice between 5- and 100 -MHz oscillators. The 5-MHz oscillator offer the lowest noise at low f because of the higher Q and of the superior stability of the 5-MHz resonator as compared with the 100-MHz ones. In some cases $\sigma_y(\tau)$ can be lower than 10^{-13} for $\tau \approx 1$ s. On the other hand, white noise is relatively high, because the white noise of the internal amplifier is raised by the high order of frequency multiplication (2×10^3) required to attain 10 GHz. 100-MHz oscillators benefit from the lower order of needed multiplication (10^2) and from the lower white noise that results from excitation of the resonator at higher power. Yet the excitation power further reduces the low-frequency stability. Even-lower noise can be obtained with a whispering-gallery-mode reference oscillator, which benefits from the high Q of the resonator. Yet in that case an oscillator close to the frequency of the source under test is necessary.

The noise limit of the delay-line measurements originates from the noise of its constituent components, chiefly the amplifier pair, converted into input phase noise with Eqs. (5) and (6). The white noise of the amplifier pair also includes the shot noise. The latter is obtained by derivation of P_λ from P_μ. Equation (12) is used, with $m=1$ and $\eta=0.6$. Three cases are considered in which the line length is 20 km, 2 km, and 200 m. The upper frequency limit comes from $f\tau=0.95$, where Eq. (5) yields a correction of 16 dB. Between $f=0.95/\tau$ and $f=1/\tau$, the output

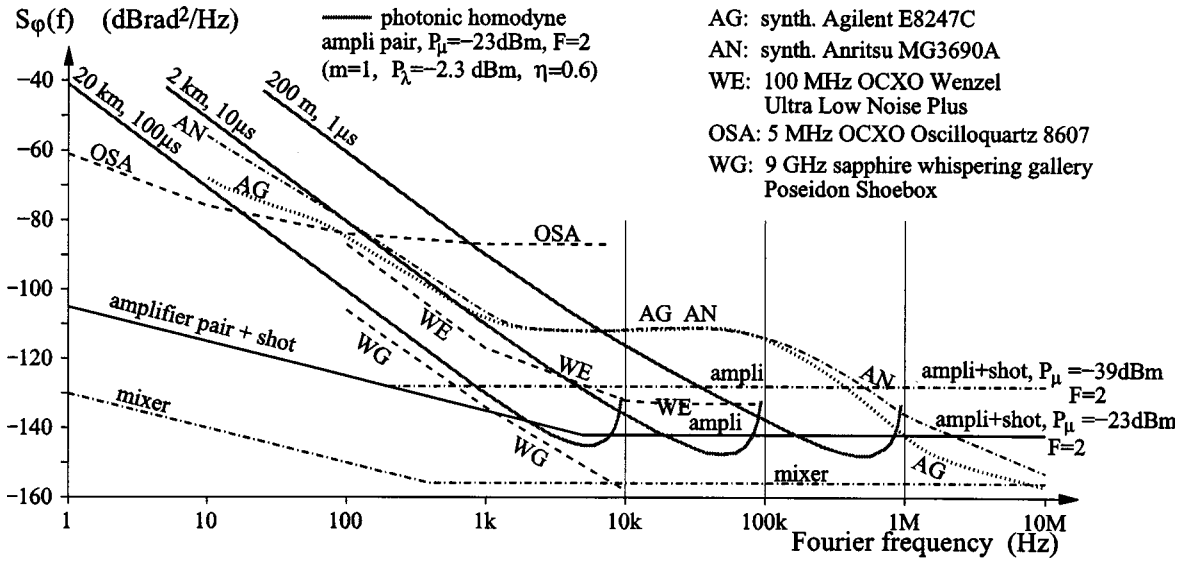

Fig. 6. Comparison between phase-noise measurement methods. The white noise of the amplifier pair also includes shot noise, calculated from the optical power that gives P_μ with $m=1$ and $\eta=0.6$.

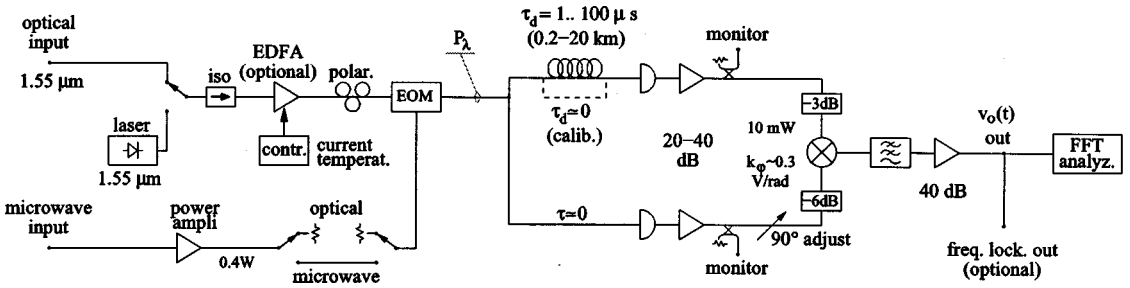

Fig. 7. Scheme of the instrument.

voltage spectrum goes abruptly to zero, where no measurement is possible.

5. MEASUREMENT OF DELAY-LINE OSCILLATORS

The background noise of the photonic homodyne instrument [Fig. 3(a)] for $f \ll 1/2\pi\tau_d$ is approximated by

$$S_{\phi i}(f) = \left(\frac{1}{2\pi\tau_d}\right)^2 \frac{1}{f^2} S_{\phi o}(f), \tag{22}$$

where $S_{\phi o}(f)$ is the overall phase noise of the optical and electrical part, chiefly the amplifier noise dominant at low f. Equation (22) is Eq. (5) inverted and approximated for low f.

Let us consider a delay-line oscillator at the frequency ν_0. Its phase noise is given by the Leeson formula[32]

$$S_{\phi l}(f) = \left[1 + \frac{\nu_0^2}{4Q^2}\frac{1}{f^2}\right] S_{\phi a}(f), \tag{23}$$

where $S_{\phi a}(f)$ is the phase noise of the sustaining amplifier and more generally the equivalent phase noise of the electronics in the loop. Taking $Q = \pi\nu_0\tau_d'$ as the equivalent merit factor of the delay line that is used as the resonator, and dropping the term "1+" in the brackets, negligible at low f, Eq. (23) becomes

$$S_{\phi l}(f) = \left(\frac{1}{2\pi\tau_d'}\right)^2 \frac{1}{f^2} S_{\phi a}(f). \tag{24}$$

Equation (24) is formally identical to Eq. (22). Hence, at first glance one may believe that the background noise of the instrument is the same as the oscillator noise [$S_{\phi i}(f) = S_{\phi l}(f)$] if the same key components are used. This means $\tau_d = \tau_d'$ for the delay line, and the same phase noise exists for the amplifier. Yet the oscillator makes use of one amplifier, whereas the instrument [Fig. 3(a)] needs two amplifiers. Thus the instrument must have either a superior amplifier technology or a longer delay line. Of course, a longer line limits the maximum f. On the other hand the design of the instrument, compared with the design of an oscillator, allows more freedom in the choosing of the most appropriate working point of all parts. Therefore it is possible to successfully design an instrument based on the same (or similar) delay and amplifier of the oscillator to be measured.

6. EXPERIMENTAL RESULTS

Figure 7 shows the complete measurement scheme. This scheme derives from Section 3 and from the experimental facts detailed in subsection 4.D. Although the instrument is mainly intended for the measurement of photonic oscillators, it is adapted to the traditional microwave oscillators by modulation of the internal 1.55-μm optical source. Phase locking, as in the traditional schemes of Fig. 2, is impossible. Yet the oscillator under test can still be frequency locked to the discriminator, which is useful for some low-noise oscillators that drift in the long term. The delay line is a Coreguide SMF28 optical fiber that exhibits an attenuation of 0.2 dB/km and a refractive index of 1.45. With a 2-km fiber, the delay is $\tau_d = 9.67$ μs. Thus the first null of $|H_\phi(f)|^2$ occurs at $f = 103.4$ kHz. The amplifier noise figure F is of ~2.5 (4 dB), which also accounts for the losses in the detector–amplifier path.

The first experiment is the measurement of a 9.9-GHz microwave source that consists of a 100-MHz quartz oscillator (Wenzel CO 233 VFW) followed by a ×99 frequency multiplier (MATS PLX32-18). The multiplier (9.9 -GHz output, +13 dBm), was connected to the microwave input of the instrument. The optical power P_λ was set to 1.7 mW, and the modulation index m was close to 1. Under these conditions, Eq. (16) predicts a noise floor of 4×10^{-15} rad^2/Hz (−144 dB rad^2/Hz). Yet P_λ and m tend to drift during the experiment, because removing the connectors and reconfiguring the circuit takes some time. This instability, due to microwave induced thermal effects in the EOM, makes the prediction of Eq. (16) rather optimistic, by an estimated factor of about two.

Figure 8 shows the results of the experiment. We first assess the residual noise of the instrument by setting $\tau_d = 0$ (the delay line is bypassed). Curve A is the residual noise of the instrument referred at the mixer input, i.e., the spectrum measured by the fast Fourier transform analyzer divided by the dc gain (40 dB) and by the mixer phase-to-voltage gain (−10 dB V/rad). The left part fits $S_\phi(f) = 4 \times 10^{-11} f^{-1}$ (−104 dB rad^2/Hz at $f = 1$ Hz). This is due to the phase flickering of the two amplifiers. Curve A has a bump at 3 kHz and also at 30 kHz, which hides the white noise floor predicted by Eq. (16). This bump is ascribed to the EDFA. A lower bump was obtained with a different EDFA. Curve B of Fig. 8 is derived from curve A by use of Eq. (5) and $\tau_d = 9.67$ μs. This is the residual noise referred to as the oscillator output, which is the instrument limit in the final measurement with the same $\tau_d = 9.67$ μs. The left part of curve B, from 10 Hz to some 2 kHz, is a frequency flicker of coefficient $b_{-3} = 1.08$

$\times 10^{-2}$. Then the delay line is restored in order to measure the oscillator noise. The phase-noise spectrum referred to as the mixer input, not shown, is converted into the oscillator noise by use of Eq. (5). This is curve C, which is fitted by the power law

$$S_\phi(f) = \frac{1.66 \times 10^{-1}}{f^3} + \frac{3 \times 10^{-4}}{f^2} + 7.7 \times 10^{-12}, \quad (25)$$

where $b_{-3} = 1.66 \times 10^{-1} = -7.7$ dB rad^2/Hz, $b_{-2} = 3 \times 10^{-4} = -35.2$ dB rad^2/Hz, and $b_0 = 7.7 \times 10^{-12} = -111.2$ dB rad^2/Hz. Flicker and white frequency noise originate in the quartz oscillator, while the white phase noise may be due to the oscillator or to the multiplier. The Allan deviation $\sigma_y(\tau)$, calculated with the conversion formulas available in Refs. 6–10, and discarding the white phase noise, is $\sigma_y = 1.25 \times 10^{-11}$ for the background noise of the instrument, and

$$\sigma_y(\tau) = 4.9 \times 10^{-11} + \frac{1.24 \times 10^{-12}}{\sqrt{\tau}} \quad (26)$$

for the oscillator under test.

Figure 9 gives an example of the reproducibility of our method. This figure refers to the same microwave source of Fig. 8, measured some six months later by a different operator after some relevant components were changed. The EOM is now a JDS Uniphase MZ-150-120-T-1-1-C2-I2-O2. The laser diode is replaced with a more powerful one (FITEL FOL 15DCWB-A81-19210-B), for the EDFA is no longer necessary. The optical power is $P_\lambda = 1.9$ mW, with a modulation index $m = 0.53$. Curves A, B, and C have the same meaning as in Fig. 8. The bumps at 3 and 30 kHz have now disappeared from curves A and B, while the flicker limit is almost unchanged. After a minimum of smoothing, the oscillator noise (curve C) overlaps to within 0.5 dB of the previous measurement.

The second experiment is the measurement of a 10.05 -GHz photonic oscillator based on a 4-km optical fiber. The 1.55-μm optical output had to be amplified from the power of 9.5 μW to 1.7 mW with the EDFA. Figure 10 shows the results. Plots A, B, and C have the same meaning and are measured in the same way as before. Curve A fits the $1/f$ line only in the frequency range from 40 Hz to less than 1 kHz and increases below 40 Hz. The residual flicker is some 5 times (7 dB) higher than in the previous case. We ascribe this phenomenon to the amplitude noise of the oscillator, taken in by the mixer. Between 20 Hz and 10 kHz, plot C (oscillator noise) is fitted by the model

$$S_\phi(f) = \frac{8 \times 10^{-1}}{f^3} + \frac{1.2 \times 10^{-3}}{f^2}, \quad (27)$$

where $b_{-3} = 0.8 = -1$ dB rad^2/Hz, $b_{-2} = 1.2 \times 10^{-3} = -29.2$ dB rad^2/Hz, which reveals the presence of flicker and white frequency noise. Below some 20 Hz, the curve C is not representative of the oscillator phase noise, because it is raised by the background noise. Converting the flicker and the white frequency noise into Allan deviation, we get

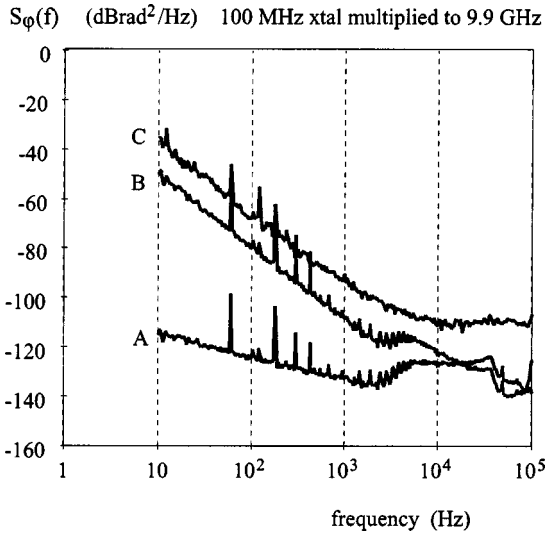

Fig. 8. Measurement of a multiplied quartz oscillator.

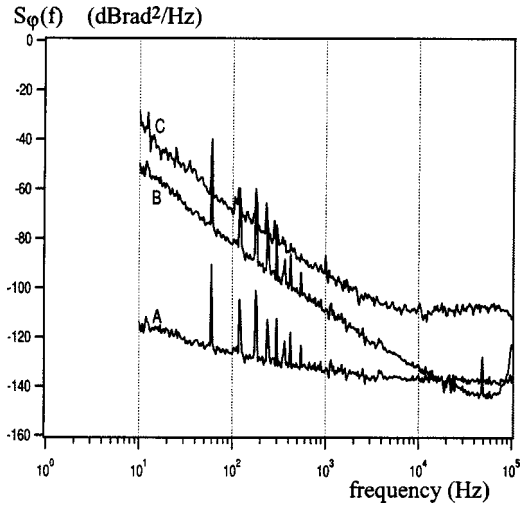

Fig. 9. Measurement of the multiplied quartz oscillator of Fig. 8, reproduced with a different experimental configuration.

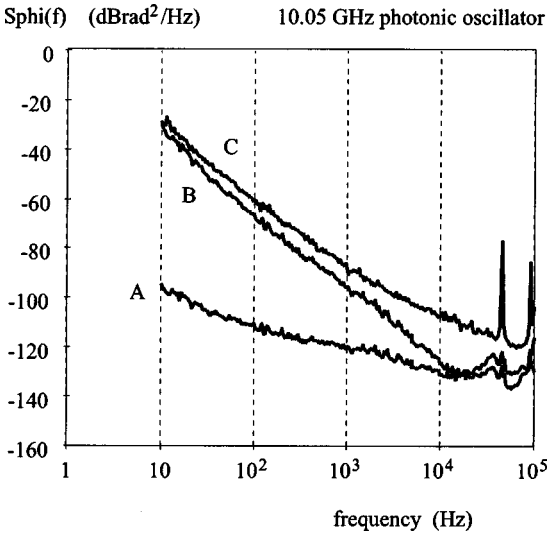

Fig. 10. Measurement of a photonic oscillator.

$$\sigma_y(\tau) = 1 \times 10^{-10} + \frac{2.4 \times 10^{-12}}{\sqrt{\tau}}. \quad (28)$$

Finally, we remark that by use of a 2-km delay line it has been possible to measure the noise of an oscillator based on a 4-km delay line, making use of similar approach and parts. This supports the conclusion of Section 5 that in practice the background noise of the instrument can often be made to be lower than the oscillator noise, if similar parts are used.

7. FINAL REMARKS

The phase-noise measurement method proposed in this paper features simplicity, straightforward implementation, and great flexibility. It is suitable for a wide range of carrier frequency (some two octaves, depending on the microwave mixer and amplifiers), it accepts either microwave or modulated optical input, and it does not require phase locking. Additionally, the presence of the optical channel enables EMI isolation and ground isolation and provides the ultimate shielding. Sensitivity, which is not the main virtue of this method, is indeed high in the 10^2-10^6 Hz region, depending on the delay used in the instrument. For example, with the use of a 20-km optical fiber (see Fig. 6) the background noise calculated in the 10^2-10^3 Hz region is 20 dB lower than the phase noise of microwave synthesizers and only 5 dB higher than that of the best commercial whispering-gallery mode oscillator.

ACKNOWLEDGMENTS

The research described in this paper was carried out at the Jet Propulsion Laboratory (JPL), California Institute of Technology, under contract of the National Aeronautics and Space Administration, and with support from Army Research Laboratory and Army Occupational Survey Program/Defense Advanced Research Projects Agency. E. Rubiola was partially supported by the Université Henri Poincaré while visiting JPL.

REFERENCES

1. X. S. Yao and L. Maleki, "Optoelectronic microwave oscillator," J. Opt. Soc. Am. B **13**, 1725–1735 (1996).
2. X. S. Yao, L. Davis, and L. Maleki, "Coupled optoelectronic oscillators for generating both RF signal and optical pulses," J. Lightwave Technol. **18**, 73–78 (2000).
3. T. A. Yilmaz, C. M. Depriest, A. Braun, J. Abeles, and P. J. Delfyett, "Noise in fundamental and harmonic modelocked semiconductor lasers: experiments and simulations," IEEE J. Quantum Electron. **39**, 838–849 (2003).
4. D. J. Jones, K. W. Holman, M. Notcutt, J. Ye, J. Chandalia, L. A. Jiang, E. P. Ippen, and H. Yokoyama, "Ultralow-jitter, 1550-nm mode-locked semiconductor laser synchronized to a visible optical frequency standard," Opt. Lett. **28**, 813–815 (2003).
5. S. T. Cundiff and J. Ye, "Colloquium: femtosecond optical frequency combs," Rev. Mod. Phys. **75**, 325–342 (2003).
6. J. Rutman, "Characterization of phase and frequency instabilities in precision frequency sources: fifteen years of progress," Proc. IEEE **66**, 1048–1075 (1978).
7. Comité Consultatif International des Radiocommunications Study Group VII, "Characterization of frequency and phase noise, Report no. 580-3," in *Standard Frequencies and Time Signals*, Vol. VII (annex) of Recommendations and Reports of the CCIR (International Telecommunication Union, Geneva, Switzerland, 1990), pp. 160–171.
8. V. F. Kroupa, ed., *Frequency Stability: Fundamentals and Measurement*. (IEEE Press, New York, 1983).
9. J. Vanier and C. Audoin, *The Quantum Physics of Atomic Frequency Standards*, (Adam Hilger, Bristol, UK, 1989), vol. 2.
10. J. R. Vig, *IEEE Standard Definitions of Physical Quantities for Fundamental Frequency and Time Metrology-Random Instabilities (IEEE Standard 1139-1999)* (IEEE, New York, 1999).
11. M. H. Hines, J. C. R. Collinet, and J. G. Ondria, "FM noise suppression of an injection phase-locked oscillator," IEEE Trans. Microwave Theory Tech. **16**, 738–742 (1968).
12. K. Kurokawa, "Noise in synchronized oscillators," IEEE Trans. Microwave Theory Tech. **16**, 234–240 (1968).
13. G. J. Dick and R. T. Wang, "Stability and phase noise tests of two cryo-cooled sapphire oscillators," IEEE Trans. Ultrason. Ferroelectr. Freq. Control **47**, 1098–1101 (2000).
14. R. A. Woode, M. E. Tobar, E. N. Ivanov, and D. Blair, "An ultra low noise microwave oscillator based on high *Q* liquid nitrogen cooled sapphyre resonator," IEEE Trans. Ultrason. Ferroelectr. Freq. Control **43**, 936–941 (1996).
15. P.-Y. Bourgeois, Y. Kersalé, N. Bazin, M. Chaubet, and V. Giordano, "Cryogenic open-cavity sapphir resonator for ultra-stable oscillator," Electron. Lett. **39**, 780–781 (2003).
16. A. L. Withwell and N. Williams, "A new microwave technique for determining noise spectra at frequencies close to the carrier," Microwave J. **2**, 27–32 (1959).
17. R. A. Campbell, "Stability measurement techniques in the frequency domain," in *Proceedings of the IEEE-NASA Symposium on Short Term Frequency Stability*, (National Aeronautics and Space Administration, Greenbelt, Md., 1964), pp. 231–235.
18. J. G. Ondria, "A microwave system for the measurement of AM and PM noise spectra," IEEE Trans. Microwave Theory Tech. **16**, 767–781 (1968).
19. R. V. Pound, "Electronic frequency stabilization of microwave oscillators," Rev. Sci. Instrum. **17**, 490–505 (1946).
20. F. Labaar, "New discriminator boosts phase noise testing," Microwaves RF **21**, 65–69 (1982).
21. A. L. Lance, W. D. Seal, and F. Labaar, "Phase noise and AM noise measurements in the frequency domain," in *Infrared and Millimeter Waves*, K. J. Button, ed., (Academic, New York, 1984), vol. 11, pp. 239–284.
22. D. Halford, A. E. Wainwright, and J. A. Barnes, "Flicker noise of phase in RF amplifiers: characterization, cause, and cure," in *Proceedings of the Frequency Control Symposium* (Institute of Electrical and Electronics Engineers, New York, 1968), pp. 340–341, abstract only.
23. F. L. Walls, E. S. Ferre-Pikal, and S. R. Jefferts, "Origin of $1/f$ PM and AM noise in bipolar junction transistor amplifiers," IEEE Trans. Ultrason. Ferroelectr. Freq. Control **44**, 326–334 (1997).
24. A. Hati, D. Howe, D. Walker, and F. Walls, "Noise figure vs. PM noise measurements: a study at microwave frequencies," in *Proceedings of the European Frequency and Time Forum & Frequency Control Symposium Joint Meeting* (Institute of Electrical and Electronics Engineers, New York, 2003).
25. E. Rubiola, E. Salik, N. Yu, and L. Maleki, "Phase noise measurement of low power signals," Electron. Lett. **39**, 1389–1390 (2003).
26. E. Rubiola and V. Giordano, "Advanced interferometric phase and amplitude noise measurements," Rev. Sci. Instrum. **73**, 2445–2457 (2002).
27. X. S. Yao and L. Maleki, "Multiloop optoelectronic oscillator," IEEE J. Quantum Electron. **36**, 79–84 (2000).
28. R. Brendel, G. Marianneau, and J. Ubersfeld, "Phase and

amplitude modulation effects in a phase detector using an incorrectly balanced mixer," IEEE Trans. Instrum. Meas. **26**, 98–102 (1977).
29. G. Cibiel, M. Régis, E. Tournier, and O. Llopis, "AM noise impact on low level phase noise measurements," IEEE Trans. Ultrason. Ferroelectr. Freq. Control **49**, 784–788 (2002).
30. W. Shieh, X. S. Yao, L. Maleki, and G. Lutes, "Phase-noise characterization of optoelectronic components by carrier suppression techniques," in *Digest of the Optical Fiber Communications Conference* (Optical Society of America, Washington, D.C., 1998), pp. 263–264.
31. A. Yariv, *Optical Electronics in Modern Communications*, 5th ed. (Oxford U. Press, New York, 1997).
32. D. B. Leeson, "A simple model of feed back oscillator noise spectrum," Proc. IEEE **54**, 329–330 (1966).